ICANS XIX,
19th meeting on Collaboration of Advanced Neutron Sources
March 8 – 12, 2010
Grindelwald, Switzerland

RESULTS FROM CAVITATION DAMAGE EXPERIMENTS WITH MERCURY SPALLATION TARGETS AT THE LANSCE – WNR IN 2008

B. W. RIEMER
Spallation Neutron Source, Oak Ridge National Laboratory[1], P.O. Box 2008
Oak Ridge, Tennessee 37831-6466, U.S.A.

and

A. ABDOU, D. K. FELDE, R. L. SANGREY, M. W. WENDEL
SNS Target Development, ORNL

ABSTRACT

Damage assessment from proton beam induced cavitation experiments on mercury spallation targets done at the LANSCE – WNR facility has been completed. The experiments investigated two key questions for the Spallation Neutron Source target, namely, how damage is affected by flow velocity in the SNS coolant channel geometry, and how damage scales with proton beam intensity at a given constant charge per pulse. With regard to the former question, prior in-beam experiments indicated that the coolant channel geometry with stagnant mercury was especially vulnerable to damage which might warrant a design change. Yet other results indicated a reduction in damage with the introduction of flow. Using a channel geometry more prototypic to the SNS, the 2008 experiment damage results show the channel is less vulnerable than the bulk mercury side of the vessel wall. They also show no benefit from increasing channel flow velocity beyond nominal SNS speeds. The second question probed a consensus belief that damage scales with beam intensity (protons per unit area) by a power law dependence with exponent of around 4. Results from a 2005 experiment did not support this power law dependence but some observations were inconsistent and unexplained. These latest results show weaker damage dependence.

1. Introduction

1.1. Background

Five mercury spallation target experiments investigating beam induced cavitation damage have been conducted at the Los Alamos Neutron Science Center – Weapons Neutron Research (LANSCE – WNR) facility since 2001 by the Spallation Neutron Source (SNS) target development team [1-3]. The principal mission of the R&D program has been development of mitigation technologies such that cavitation damage does not become the target's performance limiting issue.

The WNR facility – specifically the so-called "Blue Room" test area – is well suited to providing relevant proton beam conditions and work areas for these experiments. Proton energy is comparable to the SNS (0.8 vs. 1.0 GeV) as is pulse length (0.3 vs. 0.7 μs). Although maximum charge per pulse is about one-fifth that of SNS, by appropriately focusing the WNR beam and working with sub-SNS scale test targets, the peak beam intensity on target (protons per unit area), deposited energy density and relative energy deposition field to target geometry can be easily tailored to SNS relevant conditions. The

---

[1] ORNL/SNS is managed by UT-Battelle, LLC, for the US Department of Energy under contract DE-AC05-00OR22725.

main limitations vs. the SNS are total pulses in the test area (order 10^3 vs. 10^9) and pulse repetition rate (2 per minute vs. 60 Hz). Despite this, cavitation damage experiments at the WNR continue to provide unique and valuable data.

The irradiation phase of the most recent experiment was performed in July of 2008. A thorough description of the experiment has been provided elsewhere [4]. Preliminary results including data related to cavitation activity from external target vibrations obtained by laser Doppler vibrometer were included in [4]; reporting on passive cavitation detection by acoustic transducers is available in [5]. Damage assessment on specially polished and prepared plate specimens has taken considerable time. Following decontamination of the specimens they were examined using a 3D laser profiling microscope.

1.2. Motivation for experiment scope

The 2008 experiment campaign had two main areas of investigation. First was with regard to the SNS mercury cooling channel feature that is dedicated to removing heat from the vessel beam entrance window. Results from prior in-beam experiments using test targets with a crudely mocked-up channel indicated that channel surfaces had the most severe damage in terms of fraction of damaged area [1, 2]. While these results came from simple rectangular test target geometries with stagnant mercury, indications that the channel might be the first path of leakage were cause for concern.

Conversely, other experiment results with flowing mercury had demonstrated a reduction in damage compared to the stagnant condition [3]. Those test targets employed simple flow geometry also unlike the SNS target with the beam passing through a short depth of mercury of only 22 mm. Damage was reduced with flow to about half that compared to stagnant mercury. The test velocity was 0.5 m/s which is somewhat slower than the peak speed in the SNS channel of more than 3 m/s.

Design changes to the SNS target were contemplated to eliminate the mercury channel either by substitution with water or reconfiguring the overall mercury flow to provide vessel wall cooling from the bulk volume. Both options were conceptually feasible but would incur substantial cost and risk. Verification of the necessity of mercury channel elimination was highly desirable.

The second area of investigation was damage rate dependence on beam intensity. This issue has been under study for some time employing observations from both in-beam and off-line experiments complemented with theoretical reasoning. Indications were that damage rate dependence – specifically in the so-called incubation phase – scaled with intensity by a power law with exponent perhaps as large as 4. The implications for SNS target life at higher power are also cause for concern. However, all evidence has not been consistent [3].

2. Experiment synopsis

2.1. Channel damage vulnerability

Test targets used for investigating channel damage vulnerability were designed to be more prototypic to the SNS geometry. A scaled comparison between the so-called WFVTL (Window Flow Vulnerability Test Loop) and SNS targets is shown in Fig. 1. Test plate surfaces have to be flat in order to polish them to metallographic standards.

Mercury flowed in the 2 mm channel at peak velocities (at the beam window) summarized in Table ITable . Stagnant mercury filled the bulk region. One test condition substituted stagnant water in the channel. Beam conditions were kept as close as possible between tests. Table I includes averages of the profiles and intensities based on analysis of a fluorescing Chromox screen and integrating current transformer.

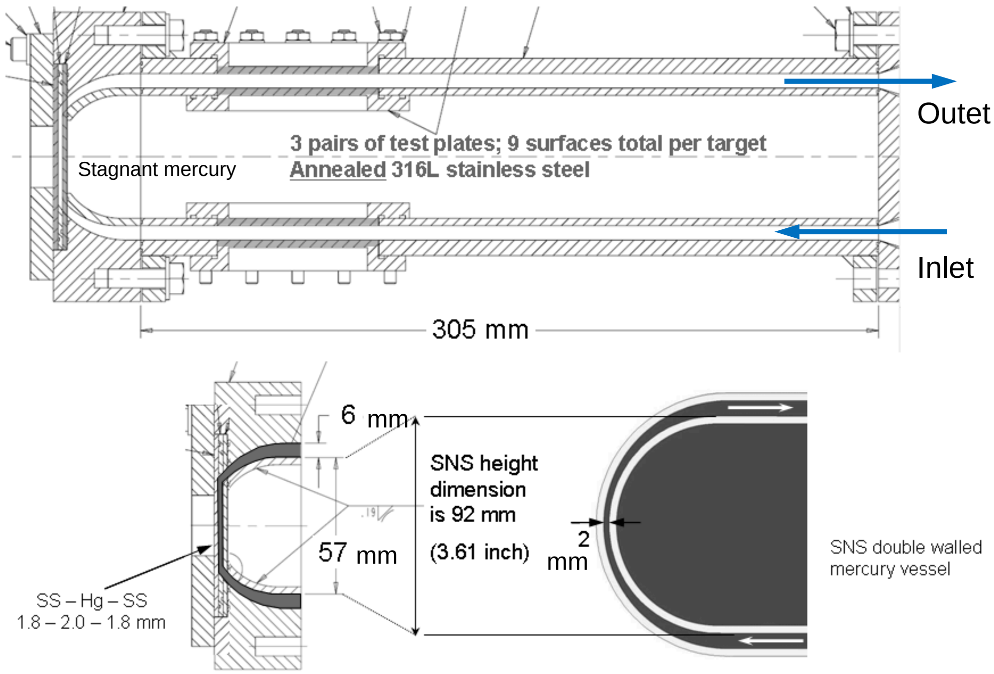

Fig. 1 Elevation cross section of WFVTL test target showing 9 test surfaces (top); test target geometry (bottom left) compared to SNS mercury vessel (bottom right), to scale.

Table I WFVTL test conditions

Test name – channel velocity	No. of Pulses	protons / pulse x 10^{12}	σ_X [mm] {half width}	σ _Y [mm] {half height}	Maximum Intensity [p/mm^2 x 10^{10}]
W0 – 0 m/s	100	26.9	18.3	7.3	3.22
W1 – 1.5 m/s	100	27.0	18.3	7.9	2.95
W2 – 4.4 m/s	100	26.8	17.4	8.0	3.07
W3 – 3 m/s	100	27.0	17.3	8.0	3.09
WW – 0 m/s (Water in channel)	100	25.9	18.5	8.4	2.66

2.2. Damage dependence on beam intensity

The target used for damage dependence on beam intensity is the same design as used in 2002 and 2005 WNR experiments. The rectangular chambers contain stagnant mercury 225 mm deep in the beam direction. Fig. 2 shows one of the targets before the front test plate was installed. Table I lists the beam parameters for this test scope. All test plate surfaces were made of annealed 316L stainless steel and polished with metallography techniques.

2.3. Gas wall with surface texture enhancement

One of the options for damage mitigation under development by the SNS R&D program is gas wall mitigation. Off-line experiments and simulations have indicated that with surface texturing on the wall gas can be encouraged to stay at the wall even under high levels of turbulence and be moved to desirable locations against adverse pressure gradients [6]. Such is the case in the SNS target bulk side of the beam entrance window. Small v-shaped grooves or conical features are particularly helpful. Here cones with a 60° included angle spaced 0.5 mm apart were tested.

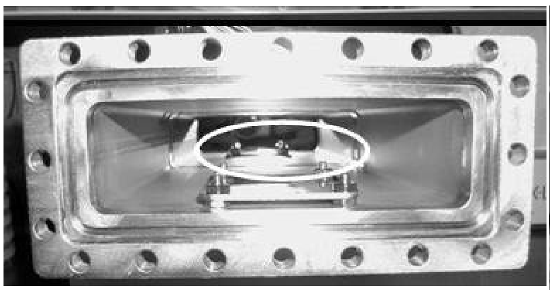

Fig. 2 Interior of rectangular target used for damage with the front (beam entrance) plate removed. A rough profile of 1-σ for the medium intensity

Fig. 3 Pre-irradiation testing of texture enhanced gas wall target with acrylic version of beam window.

Table II Beam parameters for damage dependence, textured surface and long pulse targets.

Test name – intensity	No. of Pulses	protons / pulse x 10^{12}	σ_X [mm] {half width}	σ _Y [mm] {half height}	Maximum Intensity [p/mm^2 x 10^{10}]
RH – high	100	26.5	15.4	5.2	5.25
RM – medium	100	26.6	20.2	6.1	3.43
RL – low	100	26.3	32.5	9.4	1.36
RTXT – medium (textured surface)	100	26.5	21.2	6.7	2.95
RLP – medium (long pulse)	100	45.4*	20.4	6.1	5.99

* Only one pulse charge fully captured

The term partial coverage is used to mean that gas fills the texture features but does not traverse into adjacent features. During full scale flowing tests with the SNS target configuration, partial coverage was the minimum state established over the beam spot area. Often and over a large fraction of that area the gas will traverse features as well. Because partial coverage represents a minimal protective condition it was chosen for evaluation in the WNR test.

Pre-irradiation testing of this target was done with an acrylic version of a beam window with conical type texturing as seen in Fig. 3. The light trapezoidal shaped region at the center of the window indicates partial gas coverage. Like the other rectangular targets the mercury was stagnant. During irradiation testing the coverage was refreshed prior to each beam pulse by triggering a puff of gas (helium) lasting about 2 seconds.

2.4. Long pulse test

A long pulse test was somewhat tangential to R&D program goals. However the proposed second target station at SNS is likely to be a long pulse source and there is interest in the spallation target community worldwide. LANSCE capabilities and the 2008 experiment campaign provided an opportunity. A rectangular target with stagnant mercury was employed. The beam profile for the medium intensity short pulse condition was applied and the request was for the same number of protons per pulse. The long pulses had a length of ca. 830 µs. On-line beam diagnostics failed to properly capture the charge per pulse until the last of the 100 pulses. The best evidence indicated the long pulses contained some 70% more protons per pulse than the short-pulse condition.

3. Damage Assessment Technique

A laser 3D color profile microscope was used for damage assessment of test surfaces (Keyence VK-9500). Between the WFVTL and rectangular target tests there were nearly 60 surfaces to study. Prior damage assessments from WNR experiments relied on SEM. While SEM provides detailed 2D images it does not provide the needed depth profile data. The laser microscope does not require a vacuum chamber which offers greater ease in finding the worst damage locations on a surface to study in detail.

Mirror-like polished surfaces are difficult to photograph. A method was developed to reasonably capture apparent pitting damage. These photographs – along with the discerning eye of the technician – were used to choose specific locations for image and profile data acquisition. A minimum of 5 locations were chosen for each surface for 3D scanning.

A limitation of this laser microscope is that at least a 50x objective must be used to get good quality 3D data. As a result the largest field of view for each location is 283 x 212 µm.

Processing and analysis steps of the acquired image data were done to obtain useful damage parameters. The steps for each location were:

1. Level / flatten the surface data
2. Apply modest noise filtering of the height data
3. Establish the reference height below which each identified regions were potential damaged spots
4. Export the identified features to a spreadsheet for review and compilation

Leveling is required as the specimen rarely sits exactly normal to the laser axis on the microscope stage. Establishing the reference height was a somewhat subjective step but values were chosen to maximize pit depth without having clearly non-pitting damage features (scratches or optical artifacts) be identified as potential damage.

The important damage parameters obtained from each location are maximum pit depth, damaged area fraction and mean depth of erosion. The most valuable of these given the small numbers of pulses and limited area for which data is acquired is maximum pit depth.

A final review of identified potential damage regions was manually made based on experience and judgement when looking at each features' morphology. Some identified regions were clearly defects from the polishing process, exposed defects in the material or from mishandling during decontamination. These were excluded from results.

The damage parameters were tallied for each surface from the five or more locations. Overall maximums were determined as were average values and standard deviations. Results of the tallies were then compared between surfaces and test conditions.

4. Damage results

4.1. WFVTL damage

Photographs of the front channel (beam entrance) inside surface are shown in Fig. 4 for each test velocity. The photos do not completely capture all locations of damage but were helpful for general impressions and for identifying locations to examine with the laser microscope. A horizontally oriented elliptic cluster of damage pits is apparent on all of these surfaces. The cluster appears to lessen in pit density with increasing flow. Smaller clusters of pits can be seen above and below the main group; it turns out that the deepest pits predominantly came from these smaller clusters.

Example images and profile data from two surface locations are shown in Fig. 5. The example on the left hand side is typical of a modestly damage location with the deepest features being several μm deep. The pits have a range of equivalent diameters and there were more than 30 pits distinctly identified. The right side is one of the greatest damaged locations; nearly the entire region is identified as a single pit that is 40 μm deep, even though it is apparent that multiple cavitation collapse events occurred on this region.

Fig. 6 shows the result of tallys for overall maximum pit depth for each surface. Note the change in scale for the bulk side surface due to the larger result from the front location.

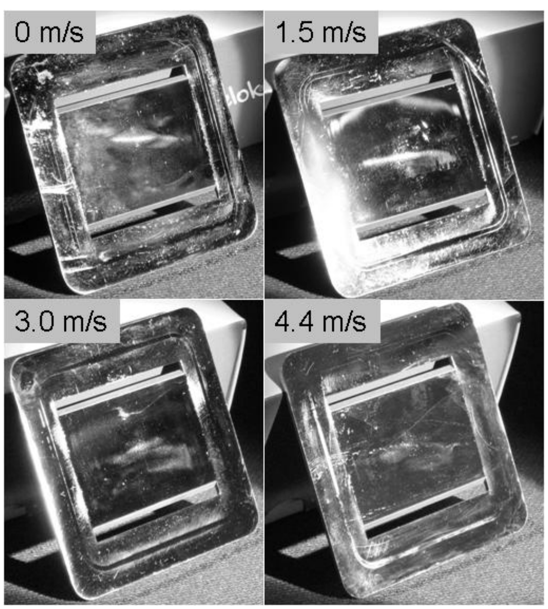

Fig. 4 Photographs of WFVTL front channel inside surfaces at 4 channel velocities.

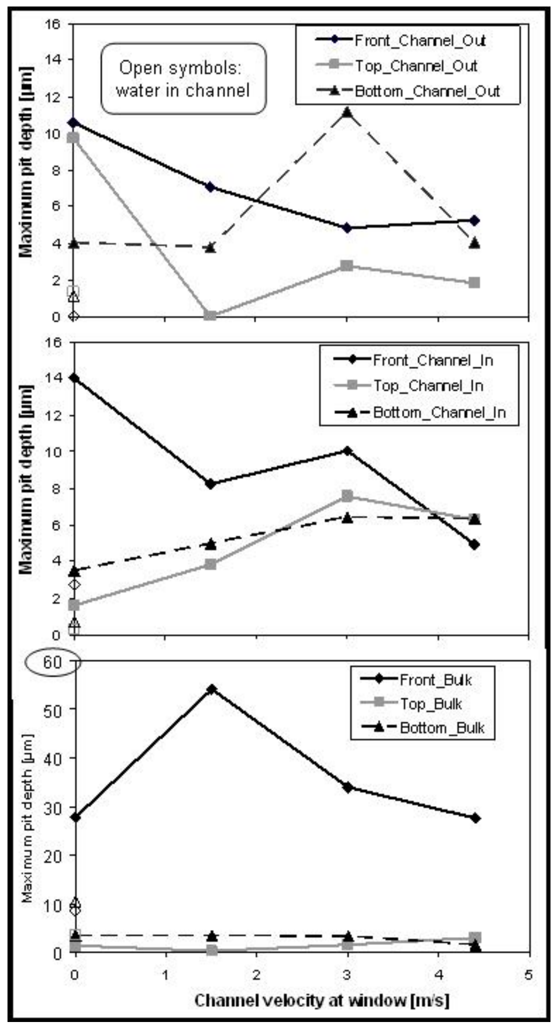

Fig. 6 Overall maximum pit depths for each test surface vs. channel flow velocity.

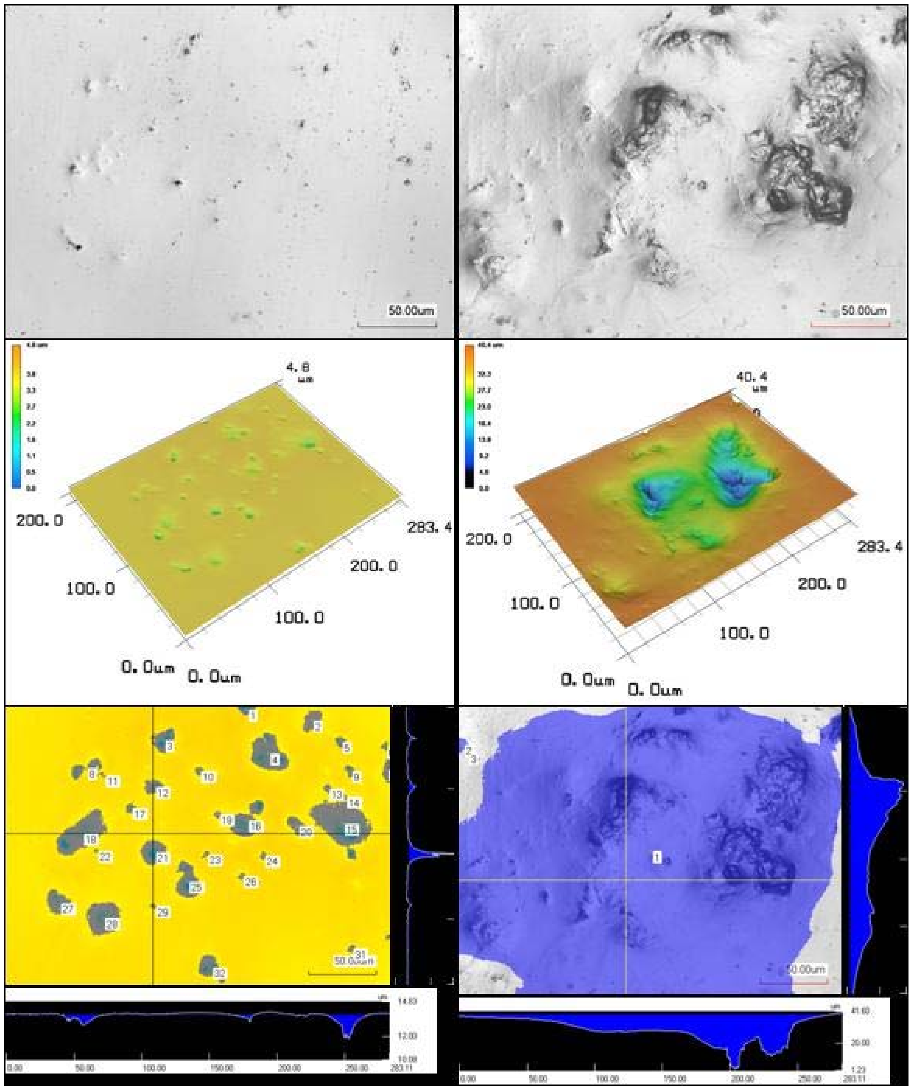

Fig. 5 Top to bottom: image, 3D profile and identified features with line profiles. Left side is bottom channel inside surface with 3.0 m/s velocity; right is front bulk side surfaces for 1.5 m/s.

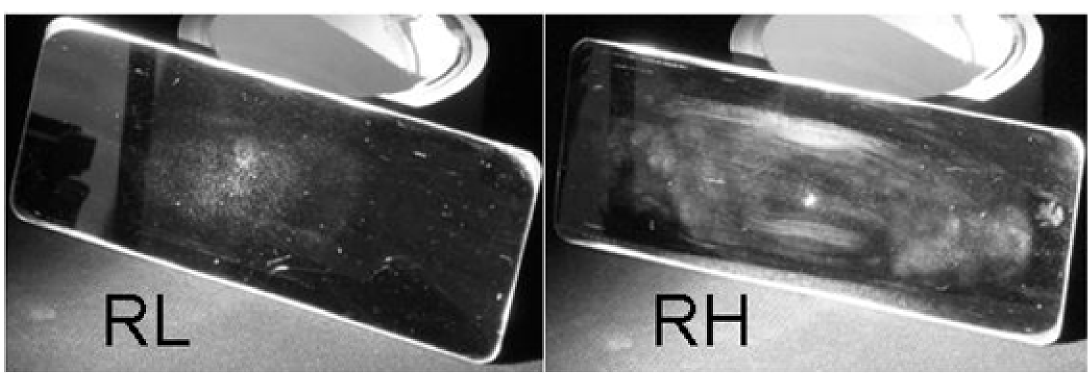

Fig. 7 Photographs of front plates from rectangular beam intensity test targets show damage on original mirror-like surfaces. Left is from low intensity beam (RL); Right is from high intensity beam (RH). Plate height and width are 64 x 165 mm.

4.2. Damage dependence on beam intensity results

Photographs of the front plates (beam entrance windows) of the low and high intensity test targets are shown in Fig. 7. The high intensity plate has a more focused spot surrounded by broad areas of cloudy regions. The low intensity plate spot is much less concentrated and cloudy regions are less apparent.

Overall maximum pit depth results for the three intensities are presented in Fig. 8 as a function of peak proton intensity per pulse (averagde results from 100 pulses each condition). Also shown is an attempted fit to the results; the power law dependency exponent is closer to 2 rather than 4.

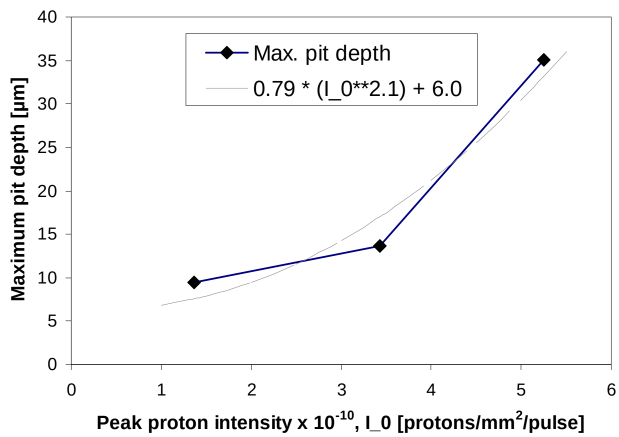

Fig. 8 Overall maximum pit depth vs. peak beam intensity along with an attempted fit of the results.

4.3. Gas wall with surface texture enhancement results

The textured surface with cones had a partial polishing process done solely to provide some regions to inspect for damage. No discernable damage could be found over this test plate.

4.4. Long pulse results

No clear evidence of cavitation damage could be found on the long pulse test plate. However there were some features that lack unequivocal explanation. Spots of cloudy regions can be seen on the long pulse surface shown on the left side of Fig. 9. Virtually all of the features are fractions of a µm deep and have pit morphologies unlike cavitation pits. The short pulse plate with the same profile is shown for comparison on the right. The central cluster of pits on the short pulse plate is not seen on the long pulse plate. There is a similar cloudy spot on the short pulse plate similar to those seen on the long pulse plate.

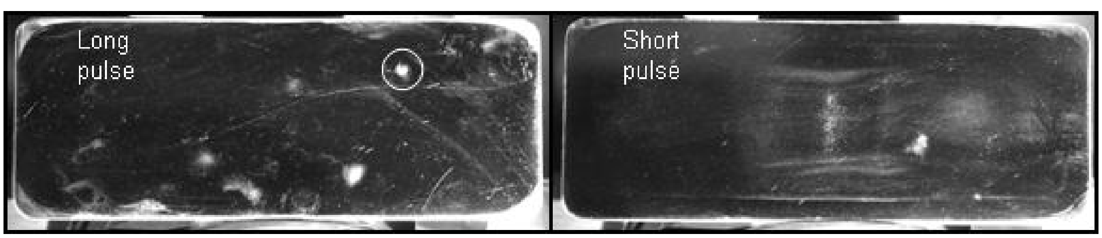

Fig. 9 Long pulse test surface on left; short pulse on right. The same beam profile was applied to both, but indications are that the long pulse had 70% greater proton fluence.

A microscope image from the circled region on the long pulse plate is shown in Fig. 10. The numerous small features are more faceted than typical caviation pits and are most likely from improper polishing. The origin of large, dark feature in the upper right is not clear. Nearby small features are more typical of material defects.

5. Summary

Damage analysis of cavitation test targets irradiated at LANSCE – WNR has been done with a 3D laser profile microscope. The obtained data was processed to provide three damage parameters, the most valuable of which is maximum pit depth.

Experiments investigating damage vulnerability of a mercury cooling channel feature of the SNS target resulted in the conclusion that the channel is not the most damage susceptible location, contrary to previous information. As a result a design change to the SNS target to eliminate this channel is not warranted.

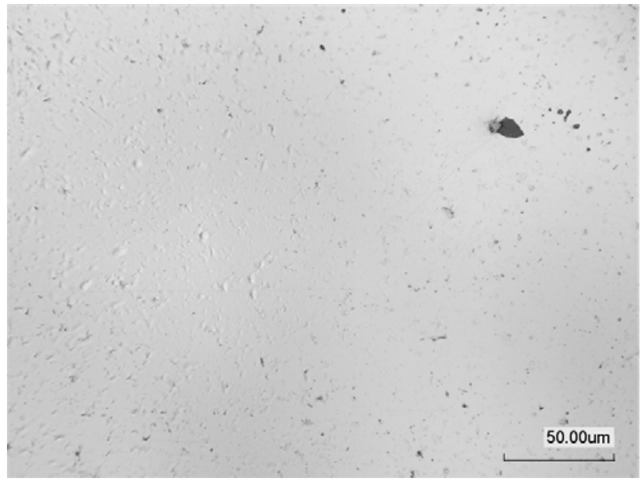

Fig. 10 Laser microscope image from cloudy spot on the long pulse test surface.

Investigation of damage rate dependence on incident proton beam intensity has shown a weaker dependence than previously believed. The results are closer to a quadradic scaling. The conducted tests varied intensity by changing beam profile while maintaining charge per pulse, i.e., they maintained the total energy on target. The experiments did nothing to refute damage dependence on intensity when profile is fixed but charge per pulse is varied. That may still scale by a power law with exponent near 4.

Gas wall mitigation with surface texturing appeared to completely prevent damage in these tests. This is an encouraging result for the SNS cavitation damage mitigation.

A long pulse test target produced no clear evidence of cavitation damage, but some observed surface features defy clear explanation.

5. Acknowledgements

This work has benefited from the use of the Los Alamos Neutron Science Center at the Los Alamos National Laboratory. This facility is funded by the US Department of Energy.

6. References

1. J.R. Haines, B.W. Riemer, D.K. Felde, J.D. Hunn, S.J. Pawel, in *J. Nucl. Mater.* **343** (2005) p. 58–69.
2. B.W. Riemer, J.R. Haines, J.D. Hunn, D.C. Lousteau, T.J. McManamy, C.C. Tsai, in *J. Nucl. Mater.* **318** (2003) 92–101.
3. B. Riemer, J. Haines, M. Wendel, G. Bauer, M. Futakawa, S. Hasegawa, H. Kogawa, in *J. Nucl. Mater.* **377** (2008) p. 162–173.
4. B.W. Riemer et al., in *J. Nucl. Mater.* **398** (2010), p. 207-219
5. N. J. Manzi, P. V. Chitnis, R.G. Holt, R.A. Roy, B. Riemer, and M. Wendel and R. O. Cleveland, “Detecting cavitation in mercury exposed to a high-energy pulsed proton beam,” in *J. Acoust. Soc. Am.* In Press (2010).
6. M.W. Wendel, D.K. Felde, A.Abdou, B.W. Riemer, “Update on Progress in Creating Stabilized Gas Layers in Flowing Liquid Mercury”, in *proceedings of ASME 2008 Fluids Engineering Division Summer Meeting*, FEDSM-78233, Vail, CO, Aug 2-5, 2009.